

duce quantum dots, rather than the external exchange gate. Based on the calculation results, optimal system configurations can be proposed for more efficient exchange energy control.

## REFERENCES

1. J.R. Petta, A.C. Johnson, J.M. Taylor, E.A. Laird, A. Yacoby, M.D. Lukin, C.M. Marcus, M.P. Hanson, and A.C. Gossard, *Science* 309, 2180 (2005).
2. P. Michler, *Quantum dots for quantum information technologies* (Berlin, Springer, 2017), vol. 237.
3. A.L. Saraiva, A. Baena, M.J. Calderon, B. Koiller, *Journ. of Phys.: Condens. Matt.* 27 (15), 154208 (2015).
4. B.E. Kane, *Nature (London)* 393, 133–137 (1998).
5. Y. He, S.K. Gorman, K. Keith, L. Kranz, J.G. Keizer, and M.Y. Simmons, *Nature* 571, 371–375 (2019).
6. Y. Makhlin, G. Schon, and A. Shnirman, *Rev. Mod. Phys.* 73, 357–400 (2001).
7. D. Loss, and D.P. DiVincenzo, *Phys. Rev. A* 57, 120 (1998).
8. J. Levy, *Phys. Rev. Lett.* 89 (14), 147902 (2002).
9. X. Hu, and S.D. Sarma, *Phys. Rev. Lett.* 96, 100501 (2006).
10. F. Baruffa, P. Stano, and J. Fabian, *Phys. Rev. B* 82 (4), 045311 (2010).
11. D.V. Melnikov, J. Kim, L.X. Zhang, and J.P. Leburton, *IEE Proceedings – Circuits, Devices and Systems* 152 (4), 377–384 (2005).
12. M.J. Calderon, A. Saraiva, B. Koiller, and S. Das Sarma, *Journ. of Appl. Phys.* 105, 122410 (2009).
13. G. Pica, B.W. Lovett, R.N. Bhatt, and S.A. Lyon, *Phys. Rev. B* 89 (23), 235306 (2014).
14. A. Kwasniowski, and J. Adamowski, *Journ. of Phys.: Cond. Matt.* 21 (23), 235601 (2009).
15. A. Fang, *Phys. Rev. B* 66, 155331 (2002).
16. Y. Wang, A. Tankasala, L.C. Hollenberg, G. Klimeck, M.Y. Simmons, and R. Rahman, *Quantum Information* 2, 16008 (2016).
17. Q. Li, L. Cywinski, D. Culcer, X. Hu, and S.D. Sarma, *Phys. Rev. B* 81, 085313 (2010).
18. W.B. Smythe, *Static and dynamic electricity* (Taylor & Francis, 1989), p. 124.
19. G.D.J. Smit, S. Rogge, J. Caro, and T.M. Klapwijk, *Phys. Rev. B* 68, 193302 (2003).

## LINEAR MAGNETORESISTANCE IN GRAPHENE FORMED ON SILICON CARBIDE: TWO DIMENSIONAL MAGNETOTRANSPORT

N. A. Poklonski<sup>1</sup>, V. A. Samuilov<sup>1,2</sup>

<sup>1)</sup> *Belarusian State University, Nezavisimosti av. 4, 220030 Minsk, Belarus*

<sup>2)</sup> *State University of New York, Department of Materials Science and Chemical Engineering  
Stony Brook, NY1179*

*Corresponding author: V. A. Samuilov (e-mail: vladimir.samuilov@stonybrook.edu)*

In this study we have tested the magnetoresistance (MR) and Hall-effect in graphene formed on semi-insulating 4H-SiC substrate by thermal decomposition of its silicon face (0001) in Ar ambient at a high temperature of 1800–2000 °C over the large areas of SiC without any passivation for checking a possibility for sensor applications. Testing was done in a relatively low magnetic fields (up to 3 T) in the temperature range from 300 to 4.2 K. A large (up to 10%) and linear magnetoresistance was observed at 300 K, which is distinctively different from the other carbon nanomaterials. Furthermore, negative magnetoresistance behavior at a low field regime for low temperatures is recognized as a weak localization in graphene. This study suggests the potential of utilizing graphene formed on semi-insulating 4H-SiC for room temperature magneto-electronic device applications and for the sensors of first order phase transitions ice–water.

**Key words:** grapheme; semi-insulating SiC; linear magnetoresistance; Hall effect; dew point; first order of phase transition detection.

## INTRODUCTION

Graphene is known as an attractive material in the development of carbon-based electronics [1–3], optical [4, 5] and magnetic devices [6, 7]. Synthesis of single- and multilayer graphene is possible either on Si-face or on C-face of SiC substrates (see for review [8]).

Individual layers in the as grown multilayer film in the C-face SiC have been found to be electronically decoupled and possess transport properties similar to a single layer graphene [9].

There is much interest in the electronic properties of single and multilayer Si-face SiC, which does not require epitaxial growth and could be attractive to the development of future commercial devices.

Usually, graphene on Si-face SiC(0001) shows low carrier 2D concentration  $n$  (of the order of magnitude  $10^{10} \text{ cm}^{-2}$ ) when being passivated with an organic film or a polymer layer [10, 11]. This type of graphene on SiC(0001) can be synthesized on a large scale by thermal decomposition of SiC(0001) in an Ar environment [12, 13].

Access to low  $n$  and the capability of growth over a large area make graphene on SiC(0001) a prominent candidate for studying graphene physics, especially near the charge neutrality point (CNP) [14].

Resistance ( $R$ ), magnetoresistance (MR) and Hall-effect study in the wide temperature ( $T$ ) range is a good characteristic of the materials in terms of the verification of the transport mechanisms of the carriers, and the material as a building block for the development of magneto-electronic devices.

## MATERIALS AND METHODS

In this work we study  $R(T)$ ,  $MR(B, T)$  and Hall-effect in graphene formed on semi-insulating 4H-SiC substrates by thermal decomposition of its silicon face (0001) in Ar ambient at a high temperature of  $\approx 1800\text{--}2000^\circ\text{C}$ .

We are not specifically looking for small coherence domains patterned into submicron structures using microelectronics lithography techniques. Instead, we have been utilizing relatively large square-shape samples (size of  $5 \times 5 \text{ mm}$ ) with the contact pads placed at the corners. The whole idea of utilizing this approach was in finding a geometry for relatively inexpensive graphene sensors.

Hall-effect was carried out in four-terminal (Van-der-Pauw) geometry in a Lake Shore Cryotronics 8400 series unit, and the  $R(T)$ ,  $MR(B, T)$  were performed in Janis ST-3T-2 helium cryostat with continuous flow, vertical  $B$  field, superconducting magnet with micro-manipulated probe station in the temperature range  $T = 4.2\text{--}300 \text{ K}$  and in magnetic fields  $B$  up to 3 T.

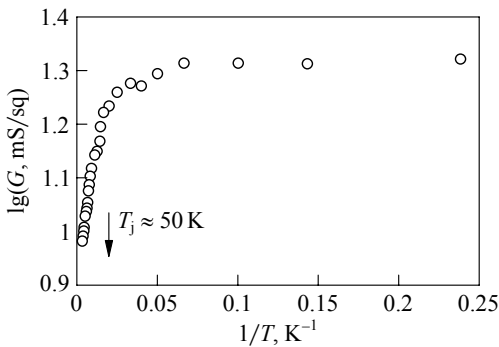
All measurements were carried out in four-terminal geometry with a constant-direct current of  $1 \mu\text{A}$ . Magnetic field was applied perpendicular to the graphene plane. We have not configured the samples for the electrostatic gating, that is why we were not able to measure the longitudinal resistance and the Hall resistivity as a function of the gate voltage.

## RESULTS AND DISCUSSION

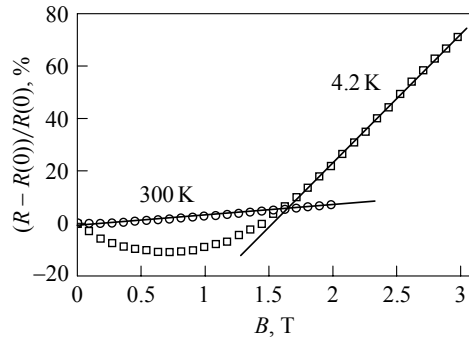
We have tested magnetoresistance (MR) and Hall-effect in low magnetic fields (up to 3 T) in the temperature range from 300 to 4.2 K. Hall data suggests *p*-type with the sheet concentration of carriers of  $\approx 3 \cdot 10^{13} \text{ cm}^{-2}$ , and relatively low mobility of  $\approx 400 \text{ cm}^2 \cdot \text{V}^{-1} \cdot \text{s}^{-1}$  for the used size of the samples of graphene.

Figure 1 shows the  $1/T$  dependence of the surface conduction  $G = 1/R$  (Arrhenius plot) with the actual  $T$  dependence starting from approximately 50 K. Following the analysis of graphene on  $\text{SiO}_2$  [4], resistance  $R$  can be defined as  $R = R_0 + R_{\text{LA}} + R_{\text{RIP}}$ , determined by the low temperature resistivity, longitudinal acoustic (LA) phonon scattering in graphene, and remote interfacial phonon (RIP) scattering by optical phonons at the surface and sub-surface of graphene, respectively [15–17]. The effect of Coulomb scattering and short-range scattering are included in  $R_0$ . At the sheet concentration of carriers of  $\approx 3 \cdot 10^{13} \text{ cm}^{-2}$ , the  $T$  dependences of Coulomb scattering and short-range scattering are thought to become feasible [16–19] but as shown in Fig. 1, resistance  $R$  is almost constant up to 50 K, which indicates their  $T$  dependences are negligible.

In the meantime, as it was found in [14], when the effect of the phonon scattering can be neglected, the major mechanism of scattering at low  $n$  up to  $\approx 5 \cdot 10^{11} \text{ cm}^{-2}$  is a Coulomb scattering and that short-range scattering becomes effective at higher carrier concentrations. That is why the resistance of the graphene sample with the high concentration of the carriers shows typical metallic behavior [20], when  $R$  increases with  $T$  at the temperatures higher than  $\approx 50 \text{ K}$ . It also was noted [21] that only metallic behavior had been observed in graphene samples at high concentrations of the carrier densities. Note, that according to Fig. 1 the temperature  $T_j \approx 50 \text{ K}$  can be a characteristic temperature of changing the mechanism of electron (or hole) transport in the graphene with point defects of structure. [According to [22], in three-dimensional semiconductors with hydrogen-like impurities (donors or acceptors), the temperature  $T_j$  characterizes the transition from the band-like to hopping conductivity of electrons or holes with respect to impurities with decreasing temperature.]



**Figure 1. – Temperature dependence of surface conduction  $G = 1/R$  of graphene sample with *p*-type carriers with sheet concentration of  $\approx 3 \cdot 10^{13} \text{ cm}^{-2}$**



**Figure 2. – The magnetoresistance (in %) of graphene formed on semi-insulating 4H-SiC at temperatures 300 and 4.2 K**

Figure 2 shows the MR (in %) at 300 and 4.2 K (intermediate temperatures are not shown) in a variable magnetic field from 0 to 3 T. We observe a linear MR with its value of  $\approx 8\%$  at 300 K at magnetic field of 2 T. This room temperature linear MR observed in our graphene is much higher than previously reported linear MR in single layer graphene [1], carbon nanotubes [2, 3], and is comparable to a recently reported value of MR in graphene nanoribbon [4]. Surprisingly, while lowering the temperature from 300 to 4.2 K, a significant increase in the slope of the linear MR and the negative MR was observed. This negative MR was found only in very low field ( $< 1.5$  T) regime at low temperatures ( $< 20$  K).

The resistance of a conductor in an applied magnetic field increases quadratically ( $MR \propto B^2$ ) [23] with the field and then saturates at a relatively low value, showing its insensitivity to the polarity of a magnetic field. Therefore, a linear MR is very interesting for magnetic sensing applications [24–26]. But, many technical challenges remain. One of them is the production of large area, high quality graphene films on Si-face of SiC, and the detailed understanding of fundamental transport in the material, with the potential of exploiting Si-face graphene for room temperature magneto-electronic and field-effect transistor applications.

We observed positive linear MR that is stable at 300 K for the magnetic field applied perpendicular to the sample surface. This linear MR was observed as a direct experimental evidence of two-dimensional (2D) magnetotransport effect in graphene [27–29], which suggests the possible origin of the linear MR behavior. In graphite, such linear MR has been observed only at low temperatures [30] suggesting that graphene is a distinctively different material. We also observed negative MR in the low field regime at low temperatures, and this negative MR was recognized as weak localization [20]; see Fig. 2.

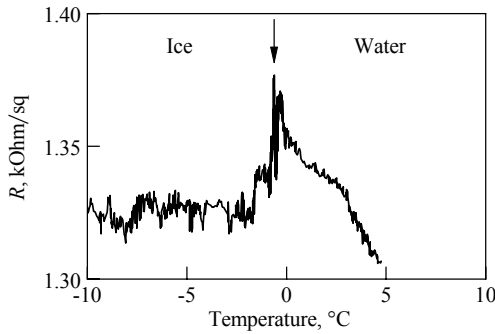


**Figure 3. – Temperature dependence of surface resistance  $R$  of graphene formed on 4H-SiC(0001) in humid atmosphere at dew point  $T_d = 2^\circ\text{C}$  while temperature is decreasing. The peak corresponds to the detection of the phase transition ice–water**

[32]). The same type of the nonmonotonous behavior was found there (see Fig. 6 in [32]). This confirms the generality of the “electric field effect” of the polar water molecules adsorption on carbon with  $sp^2$  hybridization and nonpolar ice formation at the phase transition.

Besides, testing of the temperature dependence of the resistance of our graphene material in humid atmospheres in the vicinity of the phase transition of the first order (ice–water) suggests an observation of a significant peak of the resistance vs temperature in the lambda-shape behavior (Fig. 3), which is important for the development of a new type of icing sensors [31].

In order to verify, if the phenomenon takes place specifically in graphene formed on semi-insulating 4H-SiC substrate by thermal decomposition of the (0001) silicon surface only, we did an observation of the same phenomenon on the surface of 3D sponge-like graphene material (see Fig. 5 in

## CONCLUSIONS

A large linear MR is observed in the temperature range from 300 to 4.2 K, and in the magnetic fields up to 3 T, which is distinctively different from other carbon materials. This linear MR is attributed to the two-dimensional transport in graphene on 4H-SiC. The negative MR behavior at a low field regime for low temperatures is recognized as a weak localization in graphene. Our results of large positive linear MR stable at 300 K suggest the potential of exploiting graphene on semi-insulating 4H-SiC substrates for room temperature magneto-electronic device applications.

Clear observation of the specific peaks on the temperature dependences of the resistance of graphene formed on 4H-SiC(0001) which are similar to those observed in carbon nanotube layers suggests their feasibility for utilization as inexpensive and effective sensors of icing conditions, suitable for applications in aviation and different industries.

The authors are thankful to Helava Systems and Graphene Labs for providing graphene on SiC and 3D sponge-like graphene material, and to Fernando Camino and the Proposal #43623 at the Center for Functional Nanomaterials (BNL) for help with the graphene on SiC characterization. The work was partially supported by the Belarusian National Research Program “Mattekh” and by the EU Framework Programme for Research and Innovation Horizon 2020 (Grant No. H2020-MSCA-RISE-2019-871284 SSHARE).

## REFERENCES

1. Ultrathin epitaxial graphite: 2D electron gas properties and a route toward graphene-based nanoelectronics / C. Berger [et al.] // *J. Phys. Chem. B.* – 2004. – Vol. 108, № 52. – 19912–19916.
2. Surface transfer p-type doping of epitaxial graphene / W. Chen [et al.] // *J. Am. Chem. Soc.* – 2007. – Vol. 129, № 34. – P. 10418–10422.
3. 100-GHz transistors from wafer-scale epitaxial graphene / Y.-M. Lin [et al.] // *Science.* – 2010. – Vol. 327, № 5966. – P. 662 (2010).
4. Photoresponse in epitaxial graphene with asymmetric metal contacts / R.S. Singh [et al.] // *Appl. Phys. Lett.* – 2012. – Vol. 100, № 9. – P. 093116 (3 pp.).
5. Laser patterning of epitaxial graphene for Schottky junction photodetectors / R.S. Singh [et al.] // *ACS Nano.* – 2011. – Vol. 5, № 7. – P. 5969–5975.
6. Weak antilocalization in epitaxial graphene: evidence for chiral electrons / X. Wu [et al.] // *Phys. Rev. Lett.* – 2007. – Vol. 98, № 13. – P. 136801 (4 pp.).
7. Towards a quantum resistance standard based on epitaxial graphene / A. Tzalenchuk [et al.] // *Nat. Nanotechnol.* – 2010. – Vol. 5, № 3. – P. 186–189.
8. Production and processing of graphene and related materials / C. Backes [et al.] // *2D Mater.* – 2020. – Vol. 7, № 2. – P. 022001 (282 pp.).
9. Latil, S. Massless fermions in multilayer graphitic systems with misoriented layers: Ab initio calculations and experimental fingerprints / S. Latil, V. Meunier, L. Henrard // *Phys. Rev. B.* – 2007. – Vol. 76, № 20. – P. 201402 (4 pp.).
10. Quantum oscillations and quantum Hall effect in epitaxial graphene / J. Jobst [et al.] // *Phys. Rev. B.* – 2010. – Vol. 81, № 19. – P. 195434 (6 pp.).
11. Non-volatile photochemical gating of an epitaxial graphene/polymer heterostructure / S. Lara-Avila [et al.] // *Adv. Mater.* – 2011. – Vol. 23, № 7. – P. 878–882.
12. Homogeneous large-area graphene layer growth on 6H-SiC(0001) / C. Virojanadara [et al.] // *Phys. Rev. B.* – Vol. 78, 245403 (2008).
13. Towards wafer-size graphene layers by atmospheric pressure graphitization of silicon carbide / K.V. Emtsev [et al.] // *Nat. Mater.* – 2009. – Vol. 8, № 3. – 203–207.
14. Carrier transport mechanism in graphene on SiC(0001) / S. Tanabe [et al.] // *Phys. Rev. B.* – 2011. – Vol. 84, № 11. – P. 115458 (5 pp.).

15. Intrinsic and extrinsic performance limits of graphene devices on SiO<sub>2</sub> / J.-H. Chen [et al.] // *Nat. Nanotechnol.* – 2008. – Vol. 3, № 4. – P. 206–209.
16. Carrier scattering, mobilities, and electrostatic potential in monolayer, bilayer, and trilayer graphene / W. Zhu [et al.] // *Phys. Rev. B.* – Vol. 80, № 23. – P. 235402 (8 pp.).
17. Fratini, S. Substrate-limited electron dynamics in graphene / S. Fratini, F. Guinea // *Phys. Rev. B.* – 2008. – Vol. 77, № 19. – 195415 (6 pp.).
18. Ando T. Screening effect and impurity scattering in monolayer graphene / T. Ando // *J. Phys. Soc. Jpn.* – 2006. – Vol. 75, № 7. – P. 074716 (7 pp.).
19. Hwang, E.H. Screening-induced temperature-dependent transport in two-dimensional graphene / E.H. Hwang, S. Das Sarma // *Phys. Rev. B.* – 2009. – Vol. 79, № 16. – P. 165404 (12 pp.).
20. Chapter 2.9. Structure and electron transport in irradiated monolayer graphene / I. Shlimak [et al.] // *Future trends in microelectronics. Journey into the unknown* / Ed. by S. Luryi, J. Xu, A. Zaslavsky. – New York: Wiley, 2016. – pp. 217–231.
21. Nonmonotonic temperature dependent transport in graphene grown by chemical vapor deposition / J. Heo, H.J. Chung, S.-H. Lee, H. Yang, D.H. Seo, J.K. Shin, U-In Chung, S. Seo, E.H. Hwang, S. Das Sarma // *Phys. Rev. B.* – 2011. – Vol. 84, № 3. – P. 035421 (7 pp.).
22. Transition temperature from band to hopping direct current conduction in crystalline semiconductors with hydrogen-like impurities: Heat versus Coulomb attraction / N.A. Poklonski [et al.] // *J. Appl. Phys.* – 2011. – Vol. 110, № 12. – P. 123702 (7 pp.).
23. Olsen, J.L. Electron transport in metals / J.L. Olsen. – New York: Interscience, 1962. – 121 p.
24. Magnetoresistive sensors / P.P. Freitas [et al.] // *J. Phys.: Condens. Matter.* – 2007. – Vol. 19, № 16. – P. 165221 (21 pp.).
25. Low temperature linear magnetic field sensor based on magnetoresistance of the perovskite oxide La-Sr-Co-O / R. Mahendiran [et al.] // *Rev. Sci. Instrum.* – 1995. – Vol. 66, № 4. – P. 3071–3072.
26. Weiss, H. Structure and application of galvanomagnetic devices / H. Weiss. – Oxford, Pergamon Press, 1969. – xvi+362 p.
27. Large room-temperature quantum linear magnetoresistance in multilayered epitaxial graphene: Evidence for two-dimensional magnetotransport / R.S. Singh [et al.] // *Appl. Phys. Lett.* – 2012. – Vol. 101, № 18. – P. 183105 (5 pp.).
28. Addendum: “Large room-temperature quantum linear magnetoresistance in multilayered epitaxial graphene: Evidence for two-dimensional magnetotransport” [Appl. Phys. Lett. 101, 183105 (2012)] / R.S. Singh [et al.] // *Appl. Phys. Lett.* – Vol. 103, № 4. – 2013. – P. 049902.
29. Quantum linear magnetoresistance in multilayer epitaxial graphene / A.L. Friedman [et al.] // *Nano Lett.* – 2010. – Vol. 10, № 10. – P. 3962–3965.
30. Zhang, X. Positive and negative linear magnetoresistance of graphite / X. Zhang, Q.Z. Xue, D.D. Zhu // *Phys. Lett. A.* – 2004. – Vol. 320, № 5-6. – P. 471–477.
31. Samuilov, V. Chapter 9. Electron transport in the assemblies of multiwall carbon nanotubes / V. Samuilov, J. Galibert, N. Poklonski // *Perspective of carbon nanotubes* / Ed. by H.E.D. Saleh and S.M.M. El-Sheikh. – Rijeka: IntechOpen, 2019. – P. 1–21. DOI: 10.5772/intechopen.89937.
32. Poklonski, N. Nanosensor applications of carbon nanotube films / N. Poklonski, V. Samuilov // *Proc. of VII Int. Sci. Conf. “Materials and Structures of Modern Electronics”, Minsk, 12–13 October 2016* / Editorial Board: V.B. Odzhaev (executive editor) [et al.]. – Minsk: BSU, 2016. – P. 204–207.